Inorganic Chemistry

Article

pubs.acs.org/IC

Carbene Rearrangements in Three-Coordinate N-Heterocyclic Carbene Complexes of Cobalt(II) Bis(trimethylsilyl)amide

Benjamin M. Day, Kuntal Pal, Thomas Pugh, Jessica Tuck, and Richard A. Layfield*

School of Chemistry, The University of Manchester, Oxford Road, Manchester M13 9PL, U.K.

Supporting Information

ABSTRACT: The synthesis and molecular structures of the cobalt(II) N-heterocyclic carbene (NHC) complexes $[(NHC)Co\{N(SiMe_3)_2\}_2]$, where NHC = 1,3-bis(diisopropylphenyl)-imidazolylidene (IPr) (**6**), 1,3-bis(mesityl)imidazolylidene (IMes) (**7**), and 1,3-bis(*tert*-butyl)imidazol-2-ylidene (I^tBu) (**8**), are reported. Complexes **6**–**8** are rare examples of three-coordinate cobalt NHC complexes. The steric congestion within the coordination environments of the cobalt(II) centers in **6** and **7** results in the longest Co–C(NHC) distances currently known. Investigating the thermal stability of **6**–**8**, we have found that the steric congestion in **6** is such that heating the complex to reflux in toluene prompts a rearrangement from the normal, C2-bonding mode of the IPr ligand to the corresponding "abnormal" or mesoionic bonding mode. The rearrangement results in formation of $[(aIPr)Co\{N(SiMe_3)_2\}_2]$ (**9**), which is the first cobalt complex of an abnormal NHC ligand. The Co–C bond in **9** is 0.06 Å shorter than the analogous bond in **6**, suggesting that, although the rearrangement occurs due to the spatial demands of the IPr ligand, there is also a thermodynamic driving force in terms of the Co–C bond. In contrast to the case for **6**, complex **7** is stable with respect to the normal-to-abnormal rearrangement. Refluxing complex **8** in toluene results in activation of a *tert*-butyl substituent, which is eliminated as isobutene, followed by formation of the 1-*tert*-butylimidazole complex $[(^tBuIm)Co\{N(SiMe_3)_2\}_2]$ (**10**).

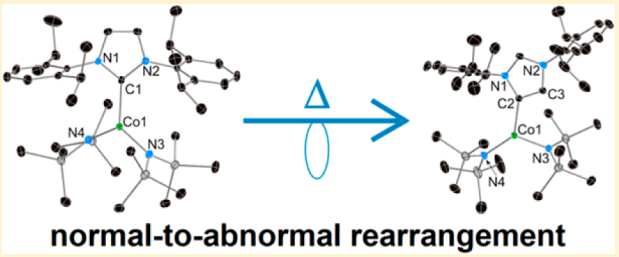

INTRODUCTION

The applications of earth-abundant metals in homogeneous catalysis have grown markedly in recent years, a trend that is driven by the desire to replace precious metals with cheaper alternatives and by the search for new reactivity.[1] Iron and cobalt have featured prominently in the development of this field, and owing to the importance of ligand design, it is unsurprising that N-heterocyclic carbene (NHC) complexes of these metals have begun to attract interest.[2,3] Although cobalt-NHC complexes have been known since the 1970s,[4] their chemistry is still underdeveloped relative to the NHC chemistry of heavier transition metals such as ruthenium, palladium, and gold.[5] Aside from the fundamental interest in cobalt-NHC chemistry, these complexes have been applied in small-molecule activation chemistry[6] and in a broad range of catalytic reactions,[7] including C–H activation.[1b]

Studies of the reactivity of iron- and cobalt-NHC complexes can be divided into two broad types—those in which the NHC complex is structurally well-defined, and those in which it is not. For the latter type, the metal-NHC complex is typically assumed to be generated in situ from some combination of a ligand precursor and a metal salt, sometimes in the presence of additives that are used to enhance reactivity. From a pragmatic perspective, catalysts generated from ill-defined mixtures of precursors present no problems if the reactivity is efficient, but if a particular reaction requires optimization, then studying the coordination chemistry becomes necessary.

Low-coordinate metal-NHC complexes have been proposed as catalytic intermediates[2] and as models for the active sites in iron-containing metalloenzymes.[8] Our own work has focused on three-coordinate iron-NHC complexes of the general type $[(NHC)Fe(N'')_2]$, where NHC = IPr (**1**), IMes (**2**), I^tBu (**3**) and N″ = $N(SiMe_3)_2$.[9,10] Complexes **1** and **3** provided some surprises that may have implications for the use of bulky NHC ligands in iron catalysis. Refluxing **1** in toluene provokes a rearrangement of the normal, C2-bound IPr ligand to its abnormal (or mesoionic) isomer $[(aIPr)Fe(N'')_2]$ (**4**). The driving force for this rearrangement is a combination of the reduction in steric pressure around the iron coordination environment with a significantly shorter and stronger Fe–C bond. Upon refluxing complex **3** in toluene for ca. 3 days, a *tert*-butyl substituent is eliminated as isobutene, and the 1-*tert*-butylimidazole complex $[(^tBuIm)_2Fe(N'')_2]$ (**5**) subsequently forms in quantitative yield.[11] In stark contrast to the case for **1** and **3**, complex **2** is stable in refluxing toluene over periods of a few days.

Having studied a series of three-coordinate iron-NHC complexes, their cobalt analogues are now considered. The chemistry of three-coordinate cobalt NHC complexes is a relatively unexplored area, and although similar behavior might be expected for NHC complexes of iron(II) and cobalt(II), this

Received: July 14, 2014
Published: September 9, 2014

dx.doi.org/10.1021/ic501677k | *Inorg. Chem.* 2014, 53, 10578–10584

cannot be assumed. Thus, we now report the synthesis and molecular structures of $[(NHC)Co(N'')_2]$, where NHC = IPr (**6**), IMes (**7**), I^{t}Bu (**8**), and investigate their thermal stability. These investigations led to the first example of a cobalt complex of an abnormal NHC ligand, $[(a\text{IPr})Co(N'')_2]$ (**9**), in addition to the three-coordinate cobalt(II) imidazole complex $[(^t\text{BuIm})\text{-}Co(N'')_2]$ (**10**).

RESULTS AND DISCUSSION

The three-coordinate complex $[(IPr)Co(N'')_2]$ (**6**) was synthesized by adding a toluene solution of IPr to a solution of cobalt(II) bis(trimethylsilyl)amide at room temperature. $[(IMes)Co(N'')_2]$ (**7**) and $[(I^tBu)Co(N'')_2]$ (**8**) were synthesized by combining the cobalt amide and the relevant NHC as solids in hexane and adding sufficient toluene to obtain homogeneous solutions (Scheme 1). The resulting dark green

Scheme 1. [a]

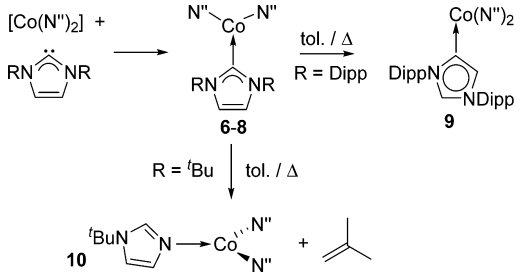

[a]NHC = IPr (**6**), IMes (**7**) and I^{t}Bu (**8**).

solutions were stirred, filtered, concentrated, and stored at −28 °C overnight, which resulted in the formation of green crystals of **6**–**8**, in good to excellent yields of 66–99%.

The molecular structures of **6**-**8** were determined by X-ray diffraction, and the key bond lengths and angles are collated in Table 1. The structure of **6** is shown in Figure 1, and those of **7** and **8** are shown in Figures S1 and S2 (Supporting Information), respectively. The three $[(NHC)Co(N'')_2]$ complexes have the common feature of a three-coordinate cobalt(II) center residing in an approximate trigonal-planar environment. Slight deviations from the ideal geometry are reflected in the range of N–Co–N and C–Co–N bond angles, which are 117.4(1)–122.7(1)° in **6**, 118.4(2)–122.8(2)° in **7**, and 111.2(2)–131.6(1)° in **8**. The N–Co–N angles are typically about 4–5° wider than the C–Co–N angles. The Co–C bond lengths to the NHC ligands are 2.119(3), 2.105(6), and 2.064(5) Å in **6**–**8**, respectively. The gradual decrease in the Co–C distance in **6**–**8** is consistent with the decrease in the steric demands of the NHC substituents,

Table 1. Selected Bond Lengths and Angles for the NHC Complexes 6–9

	6	7	8	9
Co–C/Å	2.119(3)	2.105(6)	2.064(5)	2.059(2)
Co–N(3)/Å	1.966(4)	1.952(6)	1.971(4)	1.960(2)
Co–N(4)/Å	1.958(3)	1.950(6)	1.964(5)	1.930(2)
N(3)–Co–C/deg	119.9(1)	118.7(2)	111.2(2)	104.6(1)
N(4)–Co–C/deg	117.4(1)	118.4(2)	117.2(2)	130.4(1)
N–Co–N/deg	122.7(1)	122.8(2)	131.6(2)	124.7(1)
τ/deg	49.3(3)	57.6(6)	66.1(5)	6.9(2)

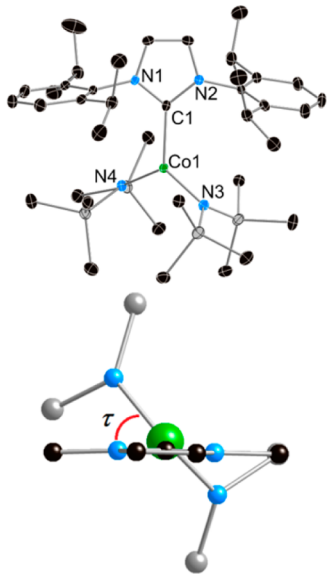

Figure 1. (top) Thermal ellipsoid representation (50% probability) of the molecular structure of **6**. Unlabeled atoms are carbon (black) and silicon (gray). Hydrogen atoms not shown. (bottom) Fragment of the structure of **6**, illustrating the torsional angle, τ.

although all three bond lengths are markedly longer than the average Co–C(NHC) distance of 1.959 Å (range 1.800–2.097 Å) in the Cambridge Structural Database,[11] and those distances in **6** and **7** are seemingly the longest Co–C(NHC) bonds currently known. The plane of the imidazolylidene C_3N_2 rings in **6**–**8** are twisted significantly with respect to the plane described by the cobalt centers and the donor atoms, with torsional angles τ (defined in Figure 1) of 49.3(3), 57.6(6), and 66.1(5)°, respectively. The increase in the torsional angle from **6** to **8** is also consistent with the decrease in the steric demands of the substituents, whereby a greater degree of freedom for rotation about the Co–C bond becomes possible with less demanding *tert*-butyl substituents.

^{1}H NMR Spectroscopy. The ^{1}H NMR spectra of **7** (Figure S4, Supporting Information) and **8** (Figure S5, Supporting Information) in toluene at 298 K consist of nonoverlapping singlet resonances and are therefore straightforward to assign. In the case of **7**, the $SiMe_3$ substituents occur at $\delta(^1H)$ −20.71 ppm, the IMes imidazolylidene protons are found at $\delta(^1H)$ +87.62 ppm, the mesityl methyl groups occur at $\delta(^1H)$ +24.49 (ortho) and −14.35 (para) ppm, and the meta aryl protons occur at $\delta(^1H)$ −13.20 ppm.

In complex **8**, the I^{t}Bu backbone protons occur at $\delta(^1H)$ +91.98 ppm, and three additional resonances, each corresponding to 18 protons, are observed in the NMR spectrum: with the aid of nuclear Overhauser experiments, this can be explained by two equivalent ^{t}Bu groups at $\delta(^1H)$ −85.83 ppm and two $N(SiMe_3)_2$ ligands in which the $SiMe_3$ substituents are nonequivalent, with $\delta(^1H)$ +32.47 and −12.69 ppm. On the basis of the solid-state molecular structure, the nonequivalence of the $SiMe_3$ substituents corresponds to one $SiMe_3$ substituent per amide ligand being oriented toward the I^{t}Bu ligand and the other being oriented away from it.

The ^{1}H NMR spectrum of **6** in toluene at 298 K (Figure S3, Supporting Information) is less straightforward but can be tentatively assigned as follows. The $SiMe_3$ groups appear as overlapping resonances at $\delta(^1H)$ −20.24 and −21.29 ppm, which is consistent with the chemical shifts determined for the

dx.doi.org/10.1021/ic501677k | Inorg. Chem. 2014, 53, 10578–10584

equivalent environments in **7** and **8**. The nonequivalence of the methyl groups in **6** is presumably a consequence of restricted rotation about the N−Si bonds due to the sterically congested coordination environment. The backbone ^{1}H environment of the IPr ligand occurs at $\delta(^1\text{H})$ +80.81 ppm, which is consistent with the analogous environments in **7** and **8**. The resonance at $\delta(^1\text{H})$ −3.04 ppm has an integral similar to that assigned to the IPr backbone environment and therefore should be due to the *p*-CH environment of the Dipp substituents. The only remaining resonance in the ^{1}H NMR spectrum of **6** with sufficient intensity to account for the methyl groups occurs at $\delta(^1\text{H})$ +17.84 ppm, and the very broad nature of this resonance could also indicate slow rotation of the isopropyl methyl groups on the NMR time scale.

In the ^{1}H NMR spectra of **6**−**8**, no evidence for dissociated NHC or for $[\text{Co}(\text{N}'')_2]_n$ (n = 1, 2) was found, which implies that the solid-state structure of each complex is retained in toluene at room temperature.

Normal-to-Abnormal Rearrangement of 6. The general structural features of $[(\text{IPr})\text{Co}(\text{N}'')_2]$ (**6**) are similar to those of $[(\text{IPr})\text{Fe}(\text{N}'')_2]$ (**1**), but one key difference is that the Co−C bond in **6** is significantly shorter, by approximately 0.063 Å, than the Fe−C bond in **1**,[10b] which is in agreement with the slightly smaller radius of cobalt(II). The shorter metal−NHC bond in **6** is not compensated for by a lengthening of metal−nitrogen distances, which are also slightly shorter, by about 0.015−0.020 Å, than the analogous distances in **1**. Given that **1** undergoes a facile rearrangement upon refluxing in toluene to the isomeric form with an abnormal IPr ligand, i.e. $[(a\text{IPr})\text{Fe}(\text{N}'')_2]$ (**4**),[9] the increased steric congestion in **6** suggests that the same type of rearrangement should occur for the cobalt analogue.

The rearrangement of **6** was first attempted on an NMR scale by heating a benzene-d_6 solution to 80 °C for 32 h, after which time a slight darkening of the green solution was observed. The ^{1}H NMR spectrum of the heated solution contains only trace amounts of **6** and features many more resonances over a broader chemical shift range of $\delta(^1\text{H})$ +163 to −22 ppm (Figure S6), indicating the formation of a cobalt complex with lower symmetry relative to the structure of **6**. To confirm that the anticipated rearrangement had occurred, the scale of the reaction was increased in order to obtain crystalline material for analysis by X-ray crystallography. After a toluene solution of **6** was refluxed for 32 h, followed by storage of the concentrated solution at −30 °C overnight, green crystals formed. The outcome of the thermolysis was subsequently revealed to be the abnormal NHC complex $[(a\text{IPr})\text{Co}(\text{N}'')_2]$ (**9**), which was isolated as a crystalline material in a moderate yield of 30%, which is probably due to the high solubility of the complex in toluene.

The molecular structure of **9** (Figure 2) features a planar, three-coordinate cobalt(II) center coordinated by two bis(trimethylsilyl)amide ligands and an abnormal (mesoionic) NHC ligand. The Co−C bond in **9** is, at 2.059(2) Å, 0.060 Å shorter than the analogous bond in the normal isomer **6**; however, the Co−N bonds in **9** are similar in length to those in **6**. Although the bond angles subtended at the cobalt center in **6** sum to approximately 360°, they span a broad range, with N(3)−Co−C, N(4)−Co−C, and N−Co−N being 104.6(1), 130.4(1), and 124.7(1)°, respectively. In contrast, the bond angles at the cobalt center in **6** span a narrower range of 117.4(1)−122.7(1)°. The asymmetric, planar three-coordinate geometry in **9** is a consequence of the significantly reduced

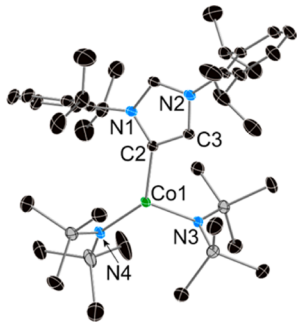

Figure 2. Thermal ellipsoid representation (50% probability) of the molecular structure of **9**. Unlabeled atoms are carbon (black) and silicon (gray). Hydrogen atoms are not shown.

steric bulk of the abnormal IPr ligand relative to its normal isomer; one of the {NDipp} units in **9** occupies a backbone position of the carbene, thus relieving steric congestion in the vicinity of the metal through a widening of the N(4)−Co−C angle.

The normal-to-abnormal rearrangement process was also investigated for $[(\text{IMes})\text{Co}(\text{N}'')_2]$ (**7**). In contrast to the case for **6**, heating solutions of **7** to reflux in toluene for up to 3 days produces no changes in the ^{1}H NMR spectrum, which reflects the stability of **7** with respect to the rearrangement and with respect to decomposition. The contrasting thermal stabilities of **6** and **7** underscore the differences in the steric demands imposed by the IPr ligand relative to those of the IMes ligand in their adducts with $[\text{Co}(\text{N}'')_2]$. This observation is broadly consistent with literature precedent, whereby complexes of the abnormal *a*IMes ligand are very rare,[12] and no structurally authenticated examples with 3d metals are known, but numerous complexes of *a*IPr-type ligands have been reported.[13,14]

Complexes **6**−**9** expand the small family of three-coordinate cobalt-NHC complexes, which includes the cobalt(I) complex $[(\text{IMes})_2\text{CoCl}]$,[3b] the NHC-stabilized cobalt(II) alkyl $[(\text{IPr})\text{Co}(\text{CH}_2\text{SiMe}_3)_2]$,[3f] and the heteroleptic cobalt(II) complexes $[(\text{NHC})\text{Co}(\text{N}'')(\text{Cl})]$ (NHC = SIMes, IMes).[3i] Three-coordinate adducts of cobalt(II) bis(trimethylsilylamide) with the general formula $[\text{LCo}(\text{N}'')_2]$ have also been reported with L = PPh_3, pyridine, thf, PCy_3, PMe_3, all of which have geometrical features similar to those of **6**−**8**.[15] In contrast to NHC complexes of 3d metals in which the carbene adopts the "normal" bonding mode, abnormal analogues are much less common, although examples are known with manganese,[16] iron,[9,10a,17] nickel,[13c] copper,[18] and zinc.[19] However, to the best of our knowledge, complex **9** is the first cobalt complex of an abnormal NHC ligand.

Thermal Decomposition of $[(\text{I}^t\text{Bu})\text{Co}(\text{N}'')_2]$ (8). Heating a benzene-d_6 solution of **8** to 80 °C in a sealed NMR tube for 24 h produces a color change from green to turquoise. The ^{1}H NMR spectrum of the turquoise solution shows no trace of complex **8**, but the resonances at $\delta(^1\text{H})$ +1.58 ppm and +4.74 ppm can be readily assigned to isobutene, which indicates that a *tert*-butyl substituent has been eliminated from the I^tBu ligand in **8** (Figure S7, Supporting Information). The prominent singlet at $\delta(^1\text{H})$ +0.09 ppm is characteristic of the trimethylsilyl groups of $(\text{Me}_3\text{Si})_2\text{NH}$, which suggests that the isobutene is generated by a deprotonation step, most likely intramolecular, although further studies would be needed to prove this. The sharp singlets at $\delta(^1\text{H})$ +34.33 and −20.91 ppm integrate in a

dx.doi.org/10.1021/ic501677k | *Inorg. Chem.* 2014, 53, 10578−10584

ratio of 9:36 and can therefore be assigned as a paramagnetically shifted ^{t}Bu substituent and the two $N(SiMe_3)_2$ ligands. The three imidazole protons are significantly deshielded and occur at $\delta(^1H)$ +240.46, +213.87, and +157.57 ppm. Reducing the solvent volume of the NMR sample resulted in the precipitation of pale blue crystals, which were shown by X-ray crystallography to be the three-coordinate 1-*tert*-butylimidazole complex $[(^t\text{BuIm})Co(N'')_2]$ (**10**) (Figure 3), the structure of

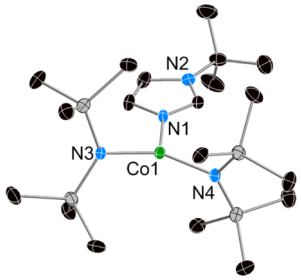

Figure 3. Thermal ellipsoid representation (50% probability) of the molecular structure of **10**. Unlabeled atoms are carbon (black) and silicon (gray). Hydrogen atoms are not shown. Selected bond lengths (Å) and angles (deg): Co(1)−N(1) 2.034(3), Co(1)−N(3) 1.921(3), Co(1)−N(4) 1.915(3); N(1)−Co(1)−N(3) 107.9(1), N(1)−Co(1)−N(4) 112.4(1), N(3)−Co(1)−N(4) 139.7(1), C(2)−N(1)−Co(1)−N(3) (τ) 12.5(3).

which is consistent with the ^{1}H NMR spectrum. The most notable contrast in the structure of **10** relative to those of **6**−**9** is the angle subtended at the cobalt center by the two amido ligands, i.e. N(3)−Co(1)−N(4), which is much wider as a consequence of the decreased steric demands of the ^{t}BuIm ligand; this is also reflected in the small τ angle of 12.5(3)°.

For comparative purposes, complex **10** was also synthesized by the straightforward addition of ^{t}BuIm to $[Co\{N(SiMe_3)_2\}_2]$; the resonances in the ^{1}H NMR spectrum of **10** obtained using this method (Figure S8, Supporting Information) occur at essentially the same chemical shifts as those due to the complex synthesized from the thermal decomposition of **8**.

Effective Magnetic Moments and UV/Vis Spectroscopy. The Evans NMR method was used to determine the effective magnetic moments of complexes **6**−**10**,[20] which lie in the range μ_{eff} = 4.7−5.1 μ_B (Table S1, Supporting Information). These values are significantly higher than the value of 3.87 μ_B predicted for S = 3/2 cobalt(II) in a three-coordinate environment with approximate C_2 symmetry, which is most likely due to the occurrence of second-order spin−orbit coupling in **6**−**10**. Similar observations have been reported previously for other three-coordinate cobalt(II) complexes.[15d]

The UV/vis spectra of 1 mM solutions of complexes **6**−**10** in hexane were recorded in the range λ 200−1000 nm. The spectra are very similar and feature a series of relatively high intensity overlapping absorptions in the region λ 242−396 nm, with an additional two absorptions for each complex with much lower intensity occurring at longer wavelengths of λ 602−750 nm (Figure S9, Supporting Information). The high-intensity absorptions at shorter wavelengths are likely to be due to charge transfer involving π-electron density on the nitrogen donor atoms and the cobalt d orbitals. The low-intensity absorptions in the visible region correspond to two of the three d−d transitions expected for high-spin cobalt(II) in a distorted C_2 ligand field. The absorption that corresponds to the third d−d transition is either so weak in intensity as to be obscured by the other two absorptions or it occurs at an energy below the lower limit of our spectrometer.

Further insight into the electronic structure of **6**−**10** was obtained from a time-dependent density functional theory (TD-DFT) study of complex **8**, which was chosen as being representative of the five three-coordinate complexes. The geometry of **8** was optimized at the B3LYP/6-311+(d,p/LANL2DZ) level of theory, assuming an electronic ground state for cobalt(II) of S = 3/2. The gas-phase optimized geometry of **8** accurately reproduces the solid-state structure, with the exception of the Co−C bond, which the DFT calculation overestimates by almost 0.11 Å (Figure S10 and Table S2, Supporting Information). Although the mismatch of the experimental and calculated Co−C bond lengths in **8** is substantial, the symmetry of the complex is preserved in the calculation, which enables a meaningful interpretation of the observed properties with DFT.

The majority of the unpaired spin in **8** resides on the cobalt(II) center, as revealed by a Mulliken spin density value of 2.70, with much smaller spin density contributions of 0.12 on the amido nitrogen atoms (Figure S11, Supporting Information). The calculated electronic excitations for **8** show that the higher-energy absorptions in the UV/vis spectrum are mostly due to various LMCT (ligand-to-metal charge transfer) transitions from the amido nitrogen π-type electron density to the cobalt d orbitals (Figure S12 and Table S4, Supporting Information). Minor contributions from MLCT and intraligand charge transfer should also contribute to the UV/vis spectrum. The lower energy absorptions in the UV/vis spectrum are consistent with d−d transitions; extending the calculation to wavelengths that are beyond the capability of our spectrometer reveals that a d−d transition at λ 1423 nm should also occur (Figures S13 and S14, Supporting Information).

CONCLUSIONS

The structures of the three-coordinate cobalt(II) NHC complexes $[(IPr)Co(N'')_2]$ (**6**), $[(IMes)Co(N'')_2]$ (**7**), and $[(I^t\text{Bu})Co(N'')_2]$ (**8**) show that steric bulk is responsible for the Co−C bonds being among the longest known in cobalt NHC complexes. In the case of **6**, the impact of the steric bulk is such that refluxing the complex in toluene provokes a normal-to-abnormal rearrangement of the IPr ligand in order to relieve steric congestion, resulting in formation of $[(a\text{IPr})Co(N'')_2]$ (**9**), in which the Co−C bond is significantly shorter than in **6**. Complex **9** is a unique example of a cobalt complex of an abnormal NHC ligand; the same rearrangement was not observed upon heating **7**, which suggests that the preparation of cobalt complexes of abnormal NHC ligands via thermolysis is probably limited to the bulkiest NHC ligands. The thermal instability of complex **8** manifests itself in the formation of isobutene and the imidazole complex $[(^t\text{BuIm})Co(N'')_2]$ (**10**). This result raises the possibility that elimination of NHC substituents as olefins may be a general reaction of cobalt complexes, particularly in situations where the coligands have basic character.

The reactivity discovered initially for the iron-NHC complexes $[(NHC)Fe(N'')_2]$ has been confirmed for the analogous cobalt complexes. Collectively, the results show that certain NHC ligands can have "noninnocent" character in iron and cobalt chemistry, which has implications for the use of these ligands in catalysis, particularly at elevated temperatures. The mechanisms through which $[(a\text{IPr})M(N'')_2]$ and

dx.doi.org/10.1021/ic501677k | *Inorg. Chem.* 2014, 53, 10578−10584

Table 2. Crystal Data and Structure Refinement Details for 6−10

	6	7	8	9	10
formula	$C_{37}H_{72}CoN_4Si_4$	$C_{33}H_{60}CoN_4Si_4$	$C_{23}H_{56}CoN_4Si_4$	$C_{37}H_{72}CoN_4Si_4$	$C_{19}H_{48}CoN_4Si_4$
formula wt	768.29	684.14	560.00	768.29	503.89
cryst syst	triclinic	tetragonal	monoclinic	monoclinic	monoclinic
space group	$P\bar{1}$	$P4_1$	$P2_1$	$P2_1/n$	$P2_1/c$
a/Å	11.2259(7)	10.9615(2)	11.3805(4)	11.9510(7)	11.2938(7)
b/Å	11.7912(7)		12.0557(4)	16.794(2)	23.6539(17)
c/Å	19.1815(19)	32.7396(8)	12.0236(4)	23.113(2)	11.9788(7)
α/deg	83.940(5)	90	90	90	90
β/deg	80.051(5)	90	96.650(3)	94.835(5)	108.216(7)
γ/deg	63.371(6)	90	90	90	90
V/Å^3	2234.4(3)	3933.80(15)	1638.54(10)	4622.5(7)	3039.7(4)
Z	2	4	2	4	4
cryst size/mm	0.3 × 0.3 × 0.2	0.8 × 0.5 × 0.3	0.4 × 0.3 × 0.3	0.6 × 0.5 × 0.5	0.2 × 0.1 × 0.01
θ range/deg	3.5−27.9	3.1−25.2	3.1−26.4	3.5−28.5	3.1−25.3
no. of rflns collected	17703	10783	12632	18514	9899
no. of indep rflns	8146	6660	6684	8455	5547
R_{int}	0.044	0.037	0.056	0.032	0.036
no. of data/restraints/params	8146/0/469	6660/1/398	6684/1/307	8455/84/495	5547/0/268
R1	0.055	0.046	0.053	0.049	0.051
wR2	0.131	0.079	0.091	0.120	0.092

$[(^t\text{BuIm})_nM(N'')_2]$ (M = Fe, Co) are formed are the subject of ongoing experimental and computational studies.

EXPERIMENTAL SECTION

General Considerations. All syntheses were carried out using standard Schlenk and glovebox techniques, using an inert atmosphere of nitrogen or argon. Toluene and hexane were dried by refluxing over potassium and sodium−potassium alloy, respectively, for at least 3 days, before being distilled and stored over activated 4 Å molecular sieves. Benzene-d_6 was distilled from molten potassium and was then stored in a glovebox over activated 4 Å molecular sieves. X-ray diffraction data for complexes **6**−**10** (Table 2) were collected on an Agilent Technologies SuperNova diffractometer, using Mo Kα radiation. Structures were solved with SHELXS using direct methods and were refined with SHELXL using least-squares minimization.[21] Compound **7** was refined as a two-component twin by applying the twin law [0,1,0,1,0,0,0,0,−1] (BASF = 0.302). The structures of **6**−**10** have been deposited in the Cambridge Structural Database, with reference codes 1013640−1013644. Literature procedures were used for the synthesis of $[Co\{N(SiMe_3)_2\}_2]_2$,[15d,22] IPr and IMes,[23] I^{t}Bu,[24] and ^{t}BuIm.[3h] NMR spectra were acquired on a Bruker 400 MHz spectrometer. UV/vis spectra were recorded as 1 mM solutions in hexane on a Camspec M501 single-beam UV/visible spectrophotometer. Elemental analyses were carried out by Mr. Stephen Boyer at London Metropolitan University, U.K.

[(IPr)Co(N″)$_2$] (6). A solution of IPr (0.27 g, 0.69 mmol) in toluene (5 mL) was added to a solution of $[Co\{N(SiMe_3)_2\}_2]_2$ (0.26 g, 0.35 mmol) in toluene (5 mL) at room temperature, and the mixture was stirred for 1 h. The resulting dark green solution was filtered and concentrated until crystalline material began to precipitate from solution. The precipitate was redissolved and the solution stored at −28 °C overnight, resulting in the formation of emerald green crystals of [(IPr)Co(N″)$_2$] (**6**) (total yield after two recrystallizations: 0.35 g, 66%). Anal. Calcd: C, 60.97; H, 9.45; N, 7.29, Found: C, 60.94, 60.97; H, 9.36, 9.38; N, 7.21, 7.27. ^{1}H NMR (benzene-d_6, δ/ppm): 80.81 (2H, IPr backbone); 17.84 (br, IPr CH_3); −3.04 (2H aryl CH); −20.24 and −21.29 (36H, $SiMe_3$). Effective magnetic moment (Evans method): μ_{eff} = 4.7 μ_B. UV/vis (nm (ε, M^{-1} cm^{-1})): 242 (1389), 308 (1095), 360 (1090), 376 (1153), 668 (79), 750 (136).

[(IMes)Co(N″)$_2$] (7). IMes (0.41 g, 1.34 mmol) and $[Co\{N(SiMe_3)_2\}_2]_2$ (0.51 g, 0.67 mmol) were combined as solids, and hexane (25 mL) was added, which produced a dark green solution and a green precipitate. The reaction mixture was stirred for 1 h and reduced to a volume of ca. 15 mL. Toluene was added dropwise until the precipitate had dissolved. The solution was filtered and stored at −28 °C overnight, resulting in the formation of emerald green crystals of [(IMes)Co(N″)$_2$] (**7**) (total yield after two recrystallizations: 0.83 g, 90%). Anal. Calcd: C, 57.94; H, 8.84; N, 8.19. Found: C, 57.81, 57.77; H, 8.63, 8.73; N, 8.06, 8.09. ^{1}H NMR (benzene-d_6, δ/ppm): 87.62 (2H, IMes backbone); 24.29 (12H, IMes o-CH_3); −13.20 (4H, aryl CH); −14.35 (6H, IMes p-CH_3); −20.71 (36H, $SiMe_3$). Effective magnetic moment (Evans method): μ_{eff} = 5.1 μ_B. UV/vis (nm (ε, M^{-1} cm^{-1})): 242 (956), 292 (745), 358 (675), 392 (881), 656 (67), 710 (125).

[(I^{t}Bu)Co(N″)$_2$] (8). The procedure was identical with that used for **7**, with I^{t}Bu (0.15 g, 0.84 mmol) and $[Co\{N(SiMe_3)_2\}_2]_2$ (0.32 g, 0.42 mmol), giving emerald green crystals of [(I^{t}Bu)Co(N″)$_2$] (**8**; 0.34 g, 72%). Anal. Calcd: C, 49.33; H, 10.08; N, 10.00. Found: C, 49.22, 49.27; H, 10.13, 10.17; N, 9.82, 9.92. ^{1}H NMR (benzene-d_6, δ/ppm): 91.98 (2H, I^{t}Bu backbone); 32.47 (18H, 2 × $SiMe_3$); −12.69 (18H, 2 × $SiMe_3$); −85.83 (18H, ^{t}Bu). Effective magnetic moment (Evans method): μ_{eff} = 4.7 μ_B. UV/vis (nm (ε, M^{-1} cm^{-1})): 242 (982), 294 (779), 358 (718), 396 (990), 646 (80), 706 (196).

[(*a*IPr)Co(N″)$_2$] (9). A solution of **6** (0.23 g, 0.30 mmol) in toluene (10 mL) was heated to reflux for 32 h, which resulted in the formation of an olive green solution. After filtration, the concentrated reaction mixture was stored at −28 °C overnight, after which time green crystals of [(*a*IPr)Co(N″)$_2$] had formed (0.07 g, 30%). Anal. Calcd: C, 60.97; H, 9.45; N, 7.29. Found: C, 58.07, 58.14; H, 9.50, 9.56; N, 6.62, 6.72. ^{1}H NMR (benzene-d_6, δ/ppm): 24.36, 13.67, −2.52, −21.11 (6H each, IPr CH_3); 163.12, 73.46, 21.37, 14.19 (1H each, p-CH and imidazolylidene CH); 50.46, 38.42, 16.38, 12.78 (2H each, m-CH and IPr C*H*Me$_2$). Effective magnetic moment (Evans method): μ_{eff} = 4.8 μ_B. UV/vis (nm (ε, M^{-1} cm^{-1})): 240 (1751), 292 (1553), 350 (1428), 608 (69) 650 (109), 700 (162).

Synthesis of [(^{t}BuIm)Co(N″)$_2$] (10) from Thermal Decomposition of [(I^{t}Bu)Co(N″)$_2$] (8). A J. Young NMR tube was charged with **8** (0.02 g, 0.4 mmol) and benzene-d_6 (0.6 mL). The resultant green solution was heated at 80 °C for 18 h, which resulted in a color change from dark green to turquoise. The NMR spectrum of the turquoise solution showed no trace of **8**, and resonances appeared at the following chemical shifts: δ(^{1}H) 35.33 (9H, ^{t}Bu), 4.74 (2H, isobutene CH_2), 1.57 (6H, isobutene CH_3), −20.91 (36H, $SiMe_3$). Slow evaporation of the solvent from the NMR tube resulted in the precipitation of pale blue crystals, which were subsequently identified by X-ray crystallography to be **8**.

dx.doi.org/10.1021/ic501677k | Inorg. Chem. 2014, 53, 10578−10584

Synthesis of [(^{t}BuIm)Co(N″)$_2$] (10). A solution of solution of 1-*tert*-butylimidazole (0.24 g, 1.93 mmol) in hexane (10 mL) was added dropwise to a solution of $[Co\{N(SiMe_3)_2\}_2]_2$ (0.73 g, 0.96 mmol) in hexane (10 mL). The resultant dark turquoise solution was stirred for 2 h before being filtered and concentrated until crystalline material began to precipitate. After the solution was gently warmed to redissolve the precipitate, it was stored at −28 °C overnight, resulting in the formation of large turquoise, platelike crystals (0.74 g, 76%). The ^{1}H NMR spectrum of complex **10** synthesized by this method is very similar to the NMR spectrum due to the complex as synthesized from the thermal decomposition of **8** (benzene-d_6, δ/ppm): 240.46, 213.87, 157.57 (1H each, imidazole CH); 34.67 (9H ^{t}Bu); −20.70 (2 × 20.70). Anal. Calcd: C, 45.29; H, 9.60; N, 11.12. Found: C, 43.16, 43.12; H, 9.57, 9.49; N, 10.68, 10.74. Effective magnetic moment (Evans method): μ_{eff} = 4.8 μ_B. UV/vis (nm (ε, M^{-1} cm^{-1})): 242 (2074), 296 (1855), 350 (1752), 602 (48), 650 (144), 692 (118).

■ ASSOCIATED CONTENT

Ⓢ Supporting Information

Figures, tables, and CIF files giving crystallographic data for **6**−**10**, ^{1}H NMR spectra, effective magnetic moment determinations, UV/vis spectra, and computational details. This material is available free of charge via the Internet at http://pubs.acs.org.

■ AUTHOR INFORMATION

Corresponding Author

*E-mail for R.A.L.: Richard.Layfield@manchester.ac.uk.

Notes

The authors declare no competing financial interest.

■ REFERENCES

(1) (a) Kovuru, G. *Chem. Rev.* **2013**, *113*, 3248. (b) Gao, K.; Yoshikai, N. *Acc. Chem. Res.* **2014**, *47*, 1208. (c) Evano, G.; Theunissen, C.; Pradal, A. *Nat. Prod. Rep.* **2013**, *30*, 1467. (d) Arrowsmith, M.; Hill, M. S.; Kociok-Köhn, G. *Chem. Eur. J.* **2013**, *19*, 2776.

(2) (a) Ingleson, M. J.; Layfield, R. A. *Chem. Commun.* **2012**, *48*, 3579. (b) Bézier, D.; Sortais, J. B.; Darcel, C. *Adv. Synth. Catal.* **2013**, *355*, 19. (c) Riener, K.; Haslinger, S.; Raba, A.; Högerl, M. P.; Cokoja, M.; Hermann, W. A.; Kühn, F. *Chem. Rev.* **2014**, *114*, 5215.

(3) (a) Mo, Z.; Liu, Y.; Deng, L. *Angew. Chem., Int. Ed.* **2013**, *52*, 10845. (b) Mo, Z.; Chen, D.; Leng, X.; Deng, L. *Organometallics* **2012**, *31*, 7040. (c) Mondal, K. C.; Samuel, P. P.; Roesky, H. W.; Carl, E.; Herbst-Irmer, R.; Stalke, D.; Schwederski, B.; Kaim, W.; Ungur, L.; Chibotaru, L. F.; Hermann, M.; Frenking, G. *J. Am. Chem. Soc.* **2014**, *134*, 1770. (d) Vélez, C. L.; Markwick, P. R. L.; Holland, R. L.; DiPasquale, A. G.; Rheingold, A. L.; O'Connor, J. M. *Organometallics* **2010**, *29*, 6695. (e) Dürr, S.; Zarzycki, B.; Ertler, D.; Ivanović-Burmazović; Radius, U. *Inorg. Chem.* **2012**, *31*, 1730. (f) Liu, X.; Pan, S.; Wu, J.; Wang, Y.; Chen, W. *Organometallics* **2013**, *32*, 209. (g) Al Thagfi, J.; Lavoie, G. G. *Organometallics* **2012**, *31*, 2463. (h) Cowley, R. E.; Bontchev, R. P.; Duesler, E. N.; Smith, J. M. *Inorg. Chem.* **2006**, *45*, 9771. (i) Danopoulos, A. A.; Braunstein, P. *Dalton Trans.* **2013**, *42*, 7276.

(4) Lappert, M. F.; Pye, P. L. *J. Chem. Soc., Dalton Trans.* **1977**, 2172.

(5) (a) Gaillard, S.; Cazin, C. S. J.; Nolan, S. P. *Acc. Chem. Res.* **2012**, *45*, 778. (b) Valente, C.; Çalimsiz, S.; Hoi, K. H.; Mallik, D.; Sayah, M.; Organ, M. G. *Angew. Chem., Int. Ed.* **2012**, *51*, 3314. (c) Samojlowicz, C.; Bieniek, M.; Grela, K. *Chem. Rev.* **2009**, *109*, 3708.

(6) (a) Hu, X.; Meyer, K. *J. Organomet. Chem.* **2005**, *690*, 5474. (b) Cowley, R. E.; Bontchev, R. P.; Sorrell, J.; Sarracino, O.; Feng, Y.; Wang, H.; Smith, J. M. *J. Am. Chem. Soc.* **2007**, *129*, 2424.

(7) (a) Ding, Z.; Yoshikai, N. *Angew. Chem., Int. Ed.* **2013**, *52*, 8574. (b) Mo, Z.; Li, Y.; Lee, H. K.; Deng, L. *Organometallics* **2011**, *30*, 4687. (c) Matsubara, K.; Sueyasu, T.; Esaki, M.; Kumamoto, A.; Nagao, S.; Yamamoto, H.; Koga, Y.; Kawata, S.; Matsumoto, T. *Eur. J. Inorg. Chem.* **2012**, 3079. (d) Gao, K.; Yoshikai, N. *J. Am. Chem. Soc.* **2013**, *135*, 9279. (e) Hatakeyama, T.; Hashimoto, S.; Ishizuka, K.; Nakamura, M. *J. Am. Chem. Soc.* **2009**, *131*, 11949. (f) Przyojski, J. A.; Arman, H. D.; Tonzetich, Z. J. *Organometallics* **2013**, *32*, 723. (g) van Rensburg, H.; Tooze, R. P.; Foster, D. F.; Slawin, A. M. Z. *Inorg. Chem.* **2004**, *43*, 2468.

(8) (a) Pulukkody, P.; Kyran, S. J.; Bethel, R. D.; Hsieh, C. H.; Hall, M. B.; Darensbourg, D. J.; Darensbourg, M. Y. *J. Am. Chem. Soc.* **2013**, *135*, 8423. (b) Hsieh, C. H.; Darensbourg, M. Y. *J. Am. Chem. Soc.* **2010**, *132*, 14118. (c) Liu, T.; Darensbourg, M. Y. *J. Am. Chem. Soc.* **2007**, *129*, 7008. (d) Deng, L.; Holm, R. H. *J. Am. Chem. Soc.* **2008**, *130*, 9878.

(9) Day, B. M.; Pugh, T.; Hendriks, D.; Fonseca Guerra, C.; Evans, D. J.; Bickelhaupt, F. M.; Layfield, R. A. *J. Am. Chem. Soc.* **2013**, *135*, 13338.

(10) (a) Pugh, T.; Layfield, R. A. *Dalton Trans.* **2014**, *43*, 4251. (b) Layfield, R. A.; McDouall, J. J. W.; Scheer, M.; Schwarzmaier, C.; Tuna, F. *Chem. Commun.* **2011**, *47*, 10623.

(11) Groom, C. R.; Allen, F. H. *Angew. Chem., Int. Ed.* **2014**, *53*, 662.

(12) (a) Lebel, H.; Janes, M. K.; Charette, A. B.; Nolan, S. P. *J. Am. Chem. Soc.* **2004**, *126*, 5046. (b) Cooke, C. E.; Jennings, M. C.; Pomeroy, R. K.; Clyburne, J. A. C. *Organometallics* **2007**, *26*, 6059. (c) Liu, Y.; Ganguly, R.; Huynh, H. V.; Leong, W. K. *Angew. Chem., Int. Ed.* **2013**, *52*, 12110.

(13) See, for example: (a) Tang, C. Y.; Smith, W.; Vidovic, D.; Thompson, A. L.; Chaplin, A. B.; Aldridge, S. *Organometallics* **2009**, *28*, 3059. (b) Campeau, L.-C.; Thansandote, P.; Fagnou, K. *Org. Lett.* **2005**, *7*, 1857. (c) Varonka, M. S.; Warren, T. H. *Organometallics* **2010**, *29*, 717.

(14) (a) Schuster, M.; Yang, L.; Raubenheimer, H. G.; Albrecht, M. *Chem. Rev.* **2009**, *109*, 3445. (b) Albrecht, M. *Chem. Commun.* **2008**, 3601. (c) Crabtree, R. H. *Coord. Chem. Rev.* **2013**, *257*, 755. (d) Arnold, P. L.; Pearson, S. *Coord. Chem. Rev.* **2007**, *251*, 596.

(15) (a) Bradley, D. C.; Hursthouse, M. B.; Smallwood, R. J.; Welch, A. J. *J. Chem. Soc. Chem. Commun.* **1972**, 872. (b) Panda, A.; Stender, M.; Olmstead, M. M.; Klavins, P.; Power, P. P. *Polyhedron* **2003**, *22*, 67. (c) Eichhöfer, A.; Lan, Y.; Mereacre, V.; Bodenstein, T.; Weigand, F. *Inorg. Chem.* **2014**, *53*, 1962. (d) Bryan, A. M.; Long, G. J.; Grandjean, F.; Power, P. P. *Inorg. Chem.* **2013**, *52*, 12152. (e) König, S. N.; Schädle, C.; Maichle-Mössmer, C.; Anwander, R. *Inorg. Chem.* **2014**, *53*, 4585. (f) König, S. N.; Schneider, D.; Maichle-Mössmer, C.; Day, B. M.; Layfield, R. A.; Anwander, R. *Eur. J. Inorg. Chem.* **2014**, DOI: 10.1002/ejic.201402557.

(16) Musgrave, R. A.; Turbervill, R. S. P.; Irwin, M.; Goicoechea. *Angew. Chem., Int. Ed.* **2012**, *51*, 10832.

(17) (a) Lavallo, V.; El-Batta, A.; Bertrand, G.; Grubbs, R. H. *Angew. Chem., Int. Ed.* **2011**, *50*, 268. (b) Danopoulos, A. A.; Tsoureas, N.; Wright, J. A.; Light, M. E. *Organometallics* **2004**, *23*, 166. (c) Musgrave, R. A.; Turbervill, R. S. P.; Irwin, M.; Herchel, R.; Goicoechea, J. M. *Dalton Trans.* **2014**, *43*, 4335.

(18) (a) Sau, S. C.; Roy, S. R.; Sen, T. K.; Mullangi, D.; Mandal, S. K. *Adv. Synth. Catal.* **2013**, *355*, 2982. (b) Hu, X.; Castro-Rodriguez, I.; Meyer, K. *Organometallics* **2003**, *22*, 3016.

(19) (a) Wang, Y.; Xie, Y.; Abraham, M. Y.; Gilliard, R. J., Jnr; Wei, P.; Campana, C. F.; Schaefer, H. F., III; von R. Schleyer, P.; Robinson, G. H. *Angew. Chem., Int. Ed.* **2012**, *51*, 10173. (b) Jochmann, P.; Stephan, D. W. *Chem. Eur. J.* **2014**, *20*, 8370. (c) Waters, J. B.; Turbervill, R. S. P.; Goicoechea, J. M. *Organometallics* **2013**, *32*, 5190. (d) Armstrong, D. R.; Baillie, S. E.; Blair, V. L.; Chabloz, N. G.; Diez, J.; Garcia-Alvarez, J.; Kennedy, A. R.; Robertson, S. D.; Hevia. *Chem. Sci.* **2013**, *4*, 4259. (e) Sen, T. K.; Sau, S. C.; Mukherjee, A.; Hota, P. K.; Mandal, S. K.; Maity, B.; Koley, D. *Dalton Trans.* **2013**, *42*, 14253.

(20) Evans, D. F. *J. Chem. Soc.* **1959**, 2003.

(21) Sheldrick, G. M. *Acta Crystallogr., Sect. A* **2008**, *A64*, 112.

(22) Bürger, H.; Wannagat, U. *Monatsh. Chem.* **1963**, *94*, 1007.

(23) Bantreil, X.; Nolan, S. P. *Nat. Protoc.* **2011**, *6*, 69.

(24) Arduengo, A. J., III; Bock, H.; Chen, H.; Denk, M.; Dixon, D. A.; Green, J. C.; Herrmann, W. A.; Jones, N. L.; Wagner, M.; West, R. *J. Am. Chem. Soc.* **1994**, *116*, 6641.